The LINNEAN SOCIETY of London BIOLOGICAL Journal of the Linnean Society

Biological Journal of the Linnean Society, 2010, **100**, 630–641. With 4 figures

Phenotypic evolution in high-elevation populations of western fence lizards (*Sceloporus occidentalis*) in the Sierra Nevada Mountains

ADAM D. LEACHÉ[1]*, DER-SHING HELMER[2] and CRAIG MORITZ[2]

[1]*Genome Center and Department of Evolution & Ecology, University of California, Davis, CA 95616, USA*
[2]*Museum of Vertebrate Zoology and Department of Integrative Biology, 3101 Valley Life Sciences Building, University of California, Berkeley, CA 94720-3160, USA*

Received 17 December 2009; revised 11 February 2010; accepted for publication 11 February 2010

Adaptive divergence in response to variable habitats, climates, and altitude is often accentuated along elevation gradients. We investigate phenotypic evolution in body size and coloration in the western fence lizard (*Sceloporus occidentalis* Baird & Girard, 1852) across elevation gradients in Yosemite National Park, California, situated in the Sierra Nevada mountains of Western North America. High-elevation populations occurring above 2100 m a.s.l. are recognized as a separate subspecies (*Sceloporus occidentalis taylori* Camp, 1916), with a distinctive phenotype characterized by a large body size and extensive blue ventral pigmentation. We sampled *S. occidentalis* from across elevation gradients in Yosemite National Park, California, and collected phenotypic data (body size and ventral coloration measurements; 410 specimens) and mitochondrial DNA sequence data (complete NADH1 gene; 969 bp, 181 specimens) to infer phylogenetic relationships, and examine the genetic and phenotypic diversity among populations. Populations of *S. occidentalis* in Yosemite National Park follow Bergmann's rule and exhibit larger body sizes in colder, high-elevation environments. The high-elevation subspecies *S. o. taylori* is not monophyletic, and the mitochondrial DNA genealogy supports a model of convergent phenotypic evolution among high-elevation populations belonging to different river drainages. The hypothesis that separate populations of *S. occidentalis* expanded up river drainages after the recession of glaciers is supported by population demographic analyses, and suggest that Bergmann's clines can evolve rapidly along elevation gradients. The distinctive high-elevation phenotype that is attributable to *S. o. taylori* has evolved independently several times, and includes adaptive phenotypic changes associated with increases in body size and ventral coloration.

ADDITIONAL KEYWORDS: Bayesian analysis – Bergmann's rule – body size – coloration – mitochondrial DNA – phylogeography – population expansion – Yosemite National Park.

INTRODUCTION

Elevation gradients offer great potential for adaptive divergence in response to changing habitats, climates, and altitude. The Sierra Nevada mountain range in Western North America extends 650 km across California, and reaches 4421 m in elevation (Storer, Usinger & Lukas, 2004). Sharp ecological and climatic transitions separate five major biotic zones, which include the foothill woodland (300–900 m), lower montane forest (900–2100 m a.s.l.), upper montane forest (2100–2750 m a.s.l.), subalpine forest (2750–2900 m a.s.l.), and alpine zone (over 2900 m a.s.l.). Numerous studies have documented examples of phylogenetic diversification in the Sierra Nevadas (Calsbeek, Thompson & Richardson, 2003; Patterson & Givnish, 2004; Rissler *et al*., 2006). Yosemite National Park, situated on the western slope of the Sierra Nevada and containing all five major biotic zones, is among the largest (3081 km^2) and least fragmented habitat blocks remaining in the Sierra Nevada, and is well-situated for studies of adaptive divergence along elevation gradients.

*Corresponding author. E-mail: aleache@ucdavis.edu

Between 1914 and 1915, the Museum of Vertebrate Zoology (MVZ) at the University of California, Berkeley, undertook a natural history survey of the Yosemite region of the Sierra Nevada, and documented a new high-elevation subspecies of the western fence lizard (*Sceloporus occidentalis* Baird & Girard, 1852) inhabiting boulder and talus slopes over 2100 m a.s.l. in the upper Merced and Tuolumne River drainages (Camp, 1916). The ventral coloration of the Sierra fence lizard (*Sceloporus occidentalis taylori* Camp, 1916) diagnoses it from all other *S. occidentalis*: specifically, adult males have extensive light-blue ventral coloration that is continuous between the chest, belly, limbs, throat, chin, and lips (Camp, 1916). In addition, high-elevation populations are larger in size compared with those occurring at lower or intermediate elevations, with adult males reaching 94 mm in snout–vent length (Smith *et al*., 1992). Although the populations of *S. occidentalis* at high elevations in the Yosemite area have distinctive phenotypes, the variation in body size and coloration could represent gradual clinal variation along an elevation gradient rather than a sharp discontinuity in phenotype.

As part of the MVZ Grinnell Resurvey Project (Moritz *et al*., 2008), we returned to Yosemite National Park between 2003 and 2005 and collected *S. occidentalis* from the same localities visited by the original MVZ expedition, in addition to new localities, to infer phylogenetic relationships, and describe genetic and phenotypic diversity, among populations distributed across elevation gradients. Evaluating genetic diversity along elevation gradients is critical in Yosemite given the recent and dramatic glacial history that has affected the region. The most recent episode of glaciation, the Tioga, peaked only 15 000–20 000 years ago, with the formation of an extensive ice field that covered the upper Tuolumne and Merced river basins, and extended down the western and southern slopes to the Yosemite and Hetch Hetchy Valley floors (Huber, 1987). Based on this geologic scenario, we predict that populations of *S. occidentalis* expanded up the Merced and Tuolumne river drainages following the thawing and receding of the glaciers. If this model of population divergence is supported, then it raises the possibility that the distinctive phenotype of *S. o. taylori* may have evolved recently and independently in separate river drainages.

MATERIAL AND METHODS

Body size and ventral coloration

We recorded phenotypic data from 410 specimens of *S. occidentalis* (177 females and 233 males; Appendix 1). For each specimen, we recorded sex and snout–vent length (SVL), and latitude, longitude, and elevation using a handheld GPS (Garmin GPS 72; geodetic datum = WGS84). We validated the elevation readings using Google Earth v.4.0.2413 (Google, Inc.). All voucher specimens and tissue samples are deposited in the MVZ (accession nos. 13817, 13957, and 14091).

To quantify ventral pigmentation, we obtained digital images of specimens (at 100 ppi) by laying them on a flatbed scanner and then uploading the images into Adobe Photoshop CS2. The total body area of each lizard, defined as the underside of the head, throat, abdomen, and vent, was selected using the lasso tool, which was measured through the 'extended histogram' reading. From the selected body outline of each individual, areas of blue, dark blue, and black were further selected for using the lasso tool. For areas of mixed black and white pigmentation, only half of the area was counted. All areas of white were ignored. Pigmented areas on the arms, legs, and tail were likewise not measured. We calculated the percentage of coloration on the ventral surface by dividing the total area of pigmentation by the total body area, and used this value in subsequent statistical tests.

After sorting the samples by sex, we then divided the samples into four groups corresponding to river drainage (Merced versus Tuolumne) and two elevation categories (high versus low), with a cut-off of 2100 m a.s.l. reflecting the minimum elevation limit of *S. o. taylori* (Camp, 1916). We excluded juvenile specimens measuring < 50 mm from our estimates of mean SVL. We tested for significant differences in body size and ventral coloration between groups using ANOVA (both one- and two-way) in Aabel 3.0.3 (Gigawiz). As the ventral coloration percentages are non-parametric, we also conducted a Kruskall–Wallis *H*-test, which has less explicit data requirements. To further ensure that the statistical tests were not negatively influenced by the inclusion of juvenile/subadult specimens, only the upper 50% quantile of body size and ventral coloration data for each group were included in the ANOVA tests.

Molecular data

We collected mitochondrial DNA sequence data from the NADH-1 (*ND1*) protein-coding gene for 181 *S. occidentalis* representing 56 localities in Yosemite National Park (Appendix 2). Individuals collected within a radius of 250 m of a single locality were pooled to condense some of the spatial extent of our population-level sampling (Chapman & Wieczorek, 2006). To amplify and sequence the *ND1* gene, we used the primers described in Leaché & Cole (2007) and a new internal primer (5′-GAACCAATCCGC CCATCATCCTC-3′). Our molecular methods follow

Leaché & Cole (2007), with the exception that we collected DNA sequences with an ABI 48-capillary 3730 DNA analyzer. All sequences are deposited in GenBank (accession nos. GU723963–GU724143).

Contiguous sequences of DNA were aligned and edited using Sequencher v.4.2. The protein coding sequences lacked any length variation. We downloaded from GenBank three additional samples of *S. occidentalis* and four closely related species within the *Sceloporus undulatus* species group to place *S. o. taylori* within a broader phylogenetic context. These samples include *S. occidentalis* (Alpine County, California: AF440021), *S. occidentalis* (San Diego County, California: AF440023), *S. occidentalis* (Jackson County, Oregon: AF440022), *Sceloporus cautus* (AF440020), *S. undulatus* (AF440083), *Sceloporus virgatus* (AF440085), *Sceloporus woodi* (AF440087), and *Sceloporus graciosus* (AF440090). We rooted our phylogenetic trees with *S. graciosus*, which is the most distantly related species in the study (Leaché, 2010).

Gene tree reconstruction

We inferred the phylogenetic relationships of all unique haplotypes using a partitioned Bayesian analysis with MrBayes v3.1.2 (Ronquist & Huelsenbeck, 2003). We separated the data into three partitions corresponding to codon positions, and tested this partitioning strategy against a model with just a single substitution model for the entire gene using Bayes factors (see Brandley *et al*. 2005). We used the Akaike information criterion in MrModeltest v2.2 (Nylander, 2004) to determine the best-fit nucleotide substitution model for each data partition. We ran four separate Bayesian analyses (each using a different starting seed) with default heating values for 10 million generations (sampling every 1000 generations). We assessed convergence by inspecting the cumulative posterior probabilities of clades using the program AWTY (Nylander *et al*. 2008). After discarding burn-in samples from the separate analyses (the first 1000 samples), we combined the remaining samples from the four separate analyses to produce a 50% majority rule consensus tree. We also constructed haplotype networks under the statistical parsimony model, with a 95% connection significance, using TCS v1.21 (Clement, Posada & Crandall, 2000).

Genetic diversity and population expansion

We calculated genetic diversity measures for high- and low-elevation populations of *S. occidentalis* in the Merced and Tuolumne river basins using Arlequin v.3.1 (Excoffier, Laval & Schneider, 2005). The genetic diversity measures include the number of polymorphic sites (s), nucleotide diversity (π; the probability that two randomly chosen homologous sites are different), and mean number of pairwise differences (k). Hierarchical analyses of molecular variance (AMOVA; Excoffier, Smouse & Quattro, 1992) were used to determine how genetic diversity is partitioned across elevation (high versus low, with a 2100 m a.s.l. cutoff), between river drainages (Merced versus Tuolumne), and between mitochondrial DNA (mtDNA) clades. AMOVA analyses were conducted using Arlequin v.3.1 (Excoffier *et al*., 2005). We also conducted Fu's test of neutrality by calculating F_s, which is also sensitive to population expansions (Fu, 1997). Large negative values of F_s indicate population expansion, but only in the absence of selection. The significance of the F_s statistic is calculated by generating a random sample under the hypothesis of population stability and selective neutrality (Excoffier *et al*., 2005). Following the simulation results of Fu (1997), we consider F_s values significant at the 5% level if their P value is below 0.02 (Fu, 1997).

To test the population expansion hypothesis further, we estimated population size (calculated as N_e, where e is effective population size) through time using Bayesian skyline plots (Drummond *et al*., 2005). An advantage of using Bayesian skyline plots for examining population demographics is that they do not require a specified demographic model (e.g. constant size, exponential growth, logistic growth, or expansive growth). We used BEAST v.1.5.3 (Drummond & Rambaut, 2007) to conduct Bayesian skyline analyses for the Merced and Tuolumne populations. We applied 10 grouped coalescent intervals and ran the analyses for 10 million generations (sampling at intervals of 1000), with the first 10% discarded as burn-in. In order to explore the timing of population expansion, we assumed a fixed 2% substitution rate per million years. Bayesian skyline reconstructions for each population were visualized using Tracer v1.4.1 (Rambaut & Drummond, 2007).

RESULTS

Body size and ventral coloration

Sceloporus occidentalis males and females are larger and have more ventral pigmentation at higher elevations in Yosemite National Park (Fig. 1; Table 1;). For males, the mean SVL at low elevations (below 2100 m a.s.l.) are 73.4 and 70.0 mm for samples from the Merced and Tuolumne rivers, respectively (Table 1). At high elevation, these average body size measurements increase to 82.0 (Merced) and 76.3 mm (Tuolumne). A similar pattern is observed for female lizards, although the overall body sizes are lower (Table 1). The maximum size recorded for any

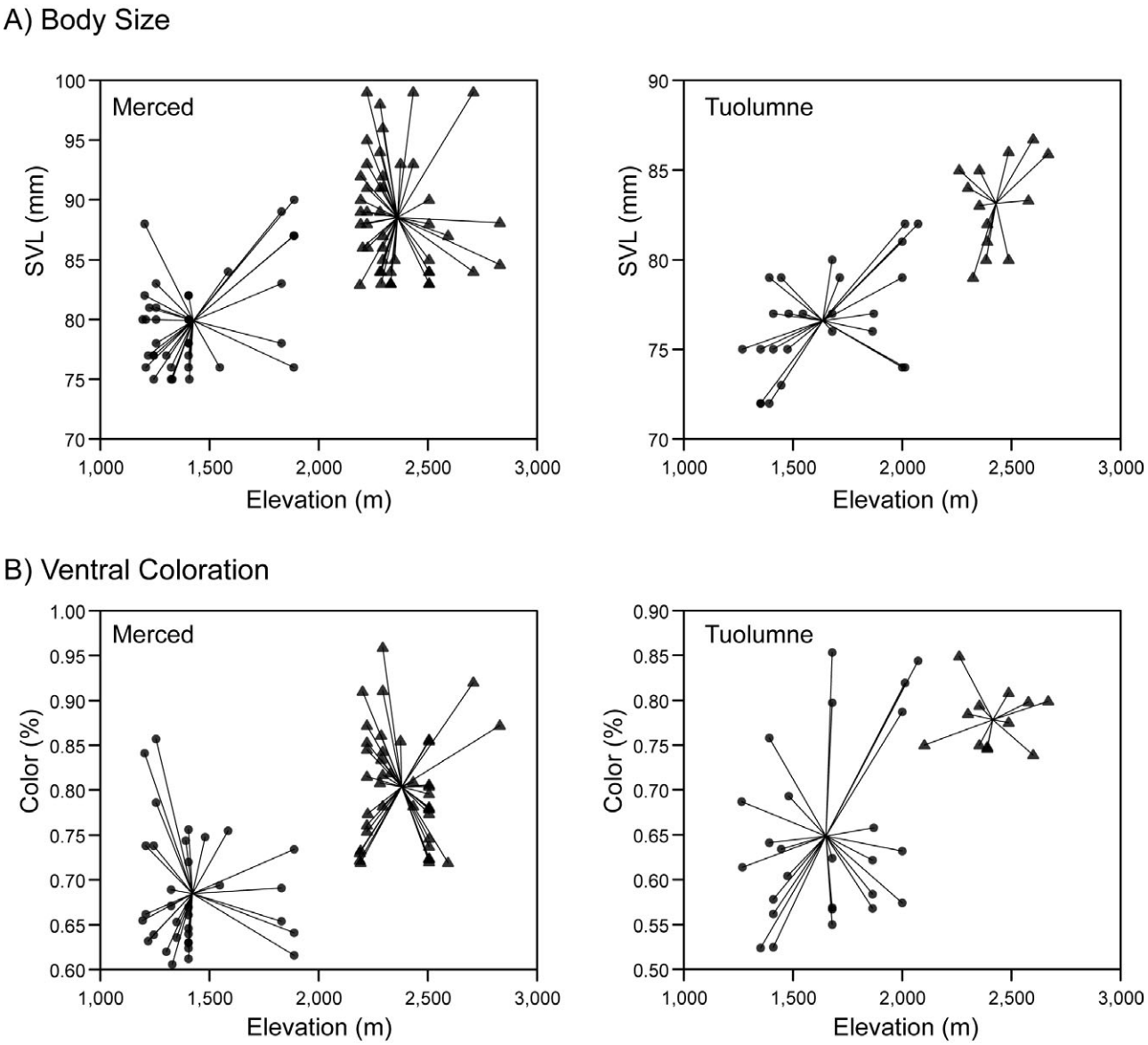

Figure 1. High-elevation populations of *Sceloporus occidentalis* in Yosemite National Park are larger in (A) body size and (B) ventral coloration versus low-elevation populations. A cut-off of 2100 m a.s.l. is used to separate populations at low elevation (circles) and high elevation (triangles). The centroid for each group represents the group mean (calculated from the upper 50% quantile).

specimen was for a male collected from the Merced Drainage measuring 99 mm SVL, whereas the largest specimen collected from low elevations measures only 90 mm SVL, and was also collected along the Merced (Table 1). The extent of blue ventral coloration in males, measured as the proportion of the ventral surface containing blue or black pigmentation, increases in high-elevation populations from a mean of 57.9 to 70.0% for Merced samples, and from 54.9 to 69.8% for Tuolumne samples (Fig. 1; Table 1). Females show a similar increase in the extent of ventral pigmentation, but the overall proportions are lower (Table 1).

The results of the ANOVA indicate that the differences in body size and coloration observed between low- and high-elevation populations of *S. occidentalis* are significant for males and females in the Merced and Tuolumne drainages ($P < 0.001$; Table 2). The differences in body size and coloration among high-elevation populations (i.e. Merced versus Tuolumne) are not significant ($P \geq 0.072$), with the exception of male body size ($P < 0.001$; Table 2). In comparisons

Table 1. Comparison of body size (snout–vent length, SVL) and ventral coloration (percentage of ventral surface containing blue/black coloration) for *Sceloporus occidentalis* collected across elevation gradients in Yosemite National Park. A cut-off value of 2100 m a.s.l. is used to separate low- and high-elevation populations. All specimens measuring ≥ 50 mm SVL are included

		Males				Females			
		Merced		Tuolumne		Merced		Tuolumne	
		Low	High	Low	High	Low	High	Low	High
Body size (SVL; mm)	Mean	73.4	82.0	70.0	76.3	68.9	75.9	68.6	74.8
	Std. Dev.	8.8	9.8	8.4	8.6	6.9	8.8	6.5	6.7
	Max.	90.0	99.0	82.0	87.0	51.0	90.0	82.0	86.0
	N	69.0	82.0	50.0	26.0	55.0	44.0	47.0	22.0
Ventral coloration (% total area)	Mean	57.9	70.0	54.9	69.8	36.3	47.9	32.1	45.6
	Std. Dev.	13.0	13.0	13.2	10.3	9.9	10.9	7.5	7.6
	Max.	85.7	95.9	85.3	84.9	73.9	78.6	56.1	68.8
	N	69.0	82.0	50.0	23.0	55.0	44.0	46.0	20.0

Table 2. ANOVA test results for comparisons of body size and ventral coloration for *Sceloporus occidentalis* from elevation gradients in Yosemite National Park. Significant *P* values are shown in bold. A cut-off value of 2100 m a.s.l. is used to separate low- and high-elevation populations

	Males		Females	
Comparison	Body size	Coloration	Body size	Coloration
One-way ANOVA				
Merced high versus Merced low	**< 0.001**	**< 0.001**	**< 0.001**	**< 0.001**
Merced high versus Tuolumne high	**< 0.001**	0.284	0.082	0.077
Merced low versus Tuolumne low	**0.003**	0.057	> 0.219	**0.004**
Tuolumne high versus Tuolumne low	**< 0.001**	**< 0.001**	**< 0.001**	**< 0.001**
Two-way ANOVA				
Elevation: high versus low	**< 0.001**	**< 0.001**	**< 0.001**	**< 0.001**
Drainage: Merced versus Tuolumne	**< 0.001**	**0.042**	**0.032**	**0.002**
Elevation + Drainage	0.222	> 0.5	0.476	> 0.5

between low-elevation populations, female body size and male ventral coloration are not significantly different ($P \geq 0.057$; Table 2). The two-way ANOVA (Table 2) also indicates that body size is significantly different between elevation ($P < 0.001$) and river drainage ($P \leq 0.042$). Results of the Kruskall–Wallis *H*-test on ventral coloration also support a significant difference between high- and low-elevation populations for males and females ($P < 0.002$), but the difference among high-elevation populations is not significantly different ($P_{\text{males}} = 0.26$; $P_{\text{females}} = 0.061$).

Phylogeny reconstruction and haplotype networks

The complete *ND1* protein-coding gene alignment (969 bp) included 182 parsimony-informative characters for the entire data set, and 94 parsimony-informative characters for *S. occidentalis*. Partitioning the data into three categories based on codon positions is favoured strongly over the unpartitioned model by the Bayes factor test (Bayes factor = 250.74).

The phylogeny provides strong support for *S. occidentalis* monophyly (Fig. 2; posterior probability = 1.0). The Yosemite samples are rendered paraphyletic by the samples of *S. occidentalis* from Alpine and San Diego Counties, California and Jackson County, Oregon, reflecting a deep phylogenetic division within Yosemite National Park (Fig. 2). Thus, two major mtDNA lineages are present in Yosemite (labelled clades A and B; Fig. 2), and strong support is provided for a subdivision of each of these clades (A1 and A2, B1 and B2; Fig. 2).

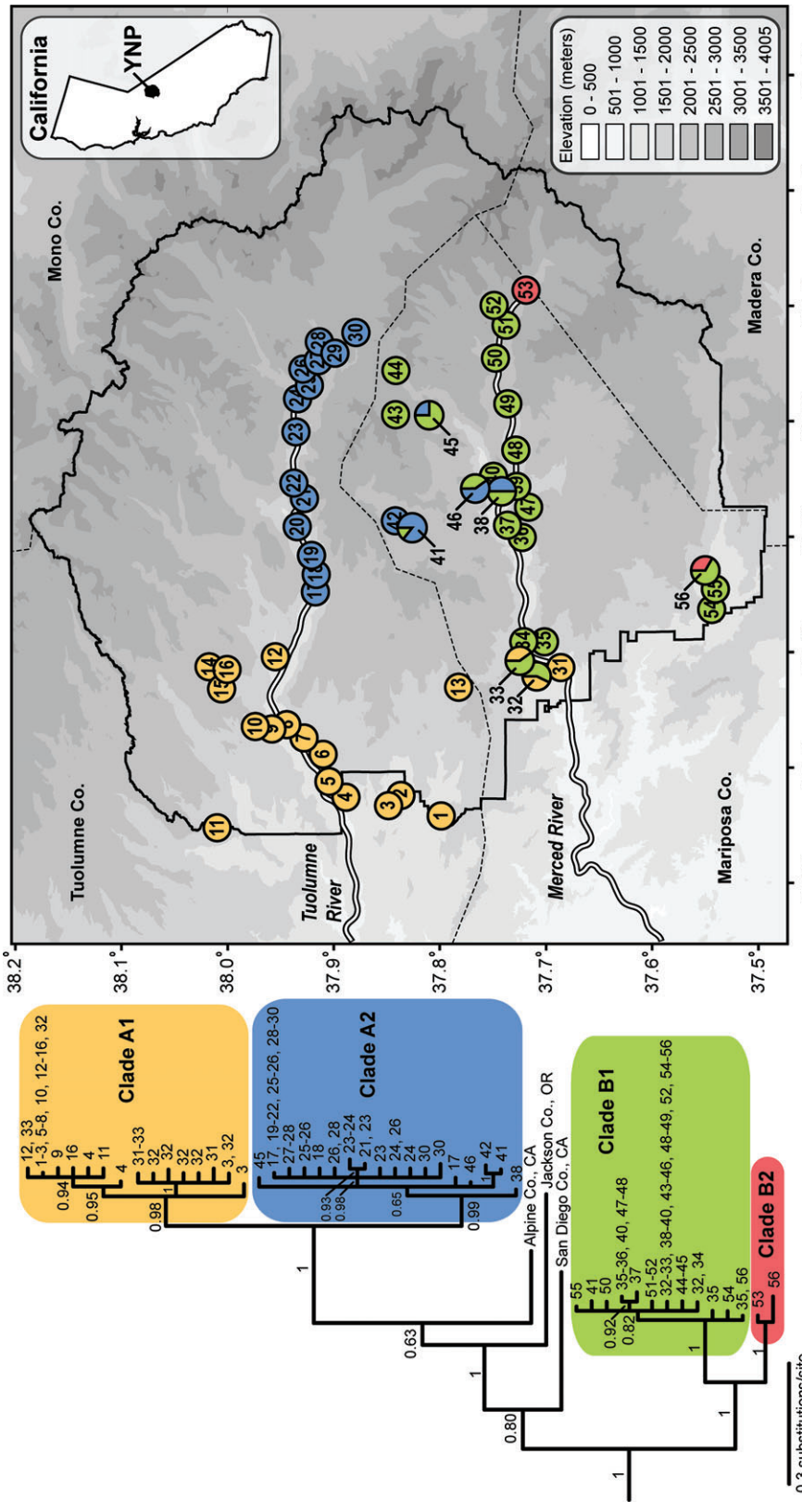

Figure 2. Mitochondrial DNA genealogy for *Sceloporus occidentalis* based on a partitioned Bayesian phylogenetic analysis. Posterior probabilities ≥ 0.50 are shown on nodes. The distributions of the major clades in Yosemite National Park are illustrated on the map, and localities with a mixture of haplotypes belonging to separate clades are indicated with pie charts.

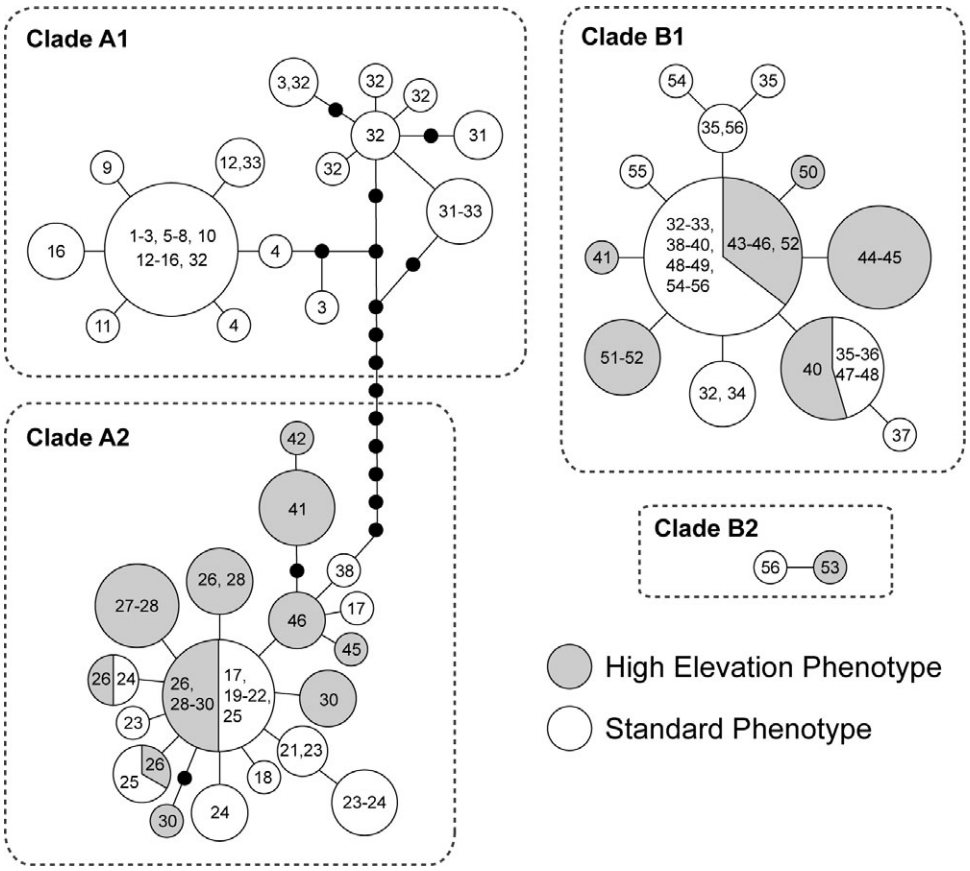

Figure 3. Haplotype networks for *Sceloporus occidentalis* constructed using statistical parsimony. Phenotypes designations are superimposed on the networks (white, standard phenotype; grey, high-elevation *Sceloporus occidentalis taylori* phenotype). Each branch is equivalent to one substitution, and black nodes represent unsampled haplotypes. The size of the circles reflects the number of sampled haplotypes. For scale, the largest circle at the centre of clade B1 contains 31 samples. Numbers correspond to the localities listed in Appendix 2.

The major mtDNA clades in Yosemite National Park are not geographically exclusive (Fig. 2). Clade A1 is distributed across low elevations on the western edge of Yosemite, and extends to mid elevations to the north and south of the Tuolumne River, but also overlaps spatially with clade B1 at low elevations along the Merced River (Fig. 2). Clade A2 is primarily distributed along the Tuolumne River from the eastern edge of the Hetch Hetchy Reservoir to high elevations, and overlaps with clade B1 at high and low elevations along the Merced River (Fig. 2). Haplotypes in clade B1 are found along the Merced River drainage from low to high elevations, and to the south in Wawona. Only two haplotypes belong to clade B2, which are found at Washburn Lake (on the edge of Madera Co.) and Wawona.

Statistical parsimony could not connect all of the haplotypes sampled from Yosemite National Park at a 95% significance level (Fig. 3). Three haplotype networks are recovered, one of which is composed of two major networks (corresponding to clades A1 and A2; Fig. 2) separated by a minimum of 11 mutational steps (Fig. 3). Mapping phenotypes onto the haplotype networks illustrates that lizards diagnosable as the high-elevation subspecies *S. o. taylori* belong to multiple mtDNA clades (i.e. clades A2, B1, and B2; Fig. 3).

Genetic diversity and population expansion

Estimates of Tamura-Nei corrected sequence divergence are low within the four mtDNA clades recovered by the phylogenetic analysis (0.11–0.52 %); however, the mean sequence divergence among clades is as high as 6.64% (Table 3). The mean sequence divergence between clades A1 and A2 is lower than that of clades B1 and B2 (1.5 versus 2.9%; Table 3). The number of segregating sites (s), nucleotide diversity (π), and mean number of pairwise differences (k) are all higher for populations distributed along the Merced River than the Tuolumne River (Table 4).

Only a small proportion (7.3%) of molecular variation occurs between high and low elevation (Table 5). By contrast, 62% occurs between river drainages (Table 5). Finally, partitioning the data by mtDNA clades distributes 89.19% of the molecular variation among populations (Table 5). Fu's F_s statistic is negative for the Tuolumne River populations, and for the high-elevation samples Fu's F_s is significantly different from zero ($P = 0.006$; Table 4). The Merced River populations have positive values for Fu's F_s, and neither value is significantly different from zero (Table 4). The Bayesian skyline plots for the Tuolumne and Merced River populations each show a recent increase in population size occurring within the last 50 000 years, assuming a substitution rate of 2% per million years (Fig. 4).

DISCUSSION

Phylogeography and taxonomy

Subspecies polyphyly is common in *Sceloporus* lizards (Wiens, Reeder & Montes De Oca, 1999; Leaché & Reeder, 2002; Leaché & Mulcahy, 2007), and *S. o. taylori* is no exception. The distinctive phenotype that characterizes the high-elevation population of *S. o. taylori* occurs in non-sister mtDNA clades that span a relatively deep node in the *S. occidentalis* phylogeny (Fig. 2). The mtDNA genealogy implies that the distinctive phenotype of *S. o. taylori* evolved rapidly in independent populations occurring in the Tuolumne and Merced river drainages over a short evolutionary timescale. This result highlights the problem associated with relying on body size and/or coloration characters to demarcate taxonomic boundaries, which are often discordant with those inferred from molecular genetic data (Burbrink, Lawson & Slowinski, 2000; Mulcahy, 2008).

The phylogenetic diversity of *S. occidentalis* in Yosemite National Park would not appear as remarkable if we had not included geographically distant samples from Oregon and other areas of California in the phylogenetic analysis. Although this additional geographic sampling is sparse (i.e. three samples), it is adequate to render the Yosemite samples polyphyletic (Fig. 2). The mtDNA genealogy gives the impres-

Table 3. Corrected sequence divergences (Tamura-Nei model) for the four mitochondrial DNA clades of *Sceloporus occidentalis* in Yosemite National Park. Numbers on the diagonal represent within-group means, and off-diagonal values are between-group means

	N	A1	A2	B1	B2
A1	46	0.298%	–	–	–
A2	61	1.531%	0.213%	–	–
B1	72	5.837%	6.123%	0.114%	–
B2	2	6.274%	6.641%	2.867%	0.519%

Table 5. Analysis of molecular variance (AMOVA) for *Sceloporus occidentalis* in Yosemite National Park. We performed three separate analyses partitioning the data into two groups.

	% Molecular variation	
Grouping	Among populations	Within populations
Elevation (2100 m a.s.l. cut-off)	7.33%	92.67%
River drainage (Merced versus Tuolumne)	62.01%	37.99%
mtDNA clade (A versus B)	89.19%	10.81%

Table 4. Genetic diversity statistics for *Sceloporus occidentalis* in Yosemite National Park. Samples are grouped by river drainage and into high- and low-elevation populations (2100 m a.s.l. cut-off). Columns show the sample size of individuals in each population, number of unique haplotypes, number of polymorphic sites (s), nucleotide diversity (π), mean number of pairwise differences (k), and Fu's F_s statistic. Significant P values are indicated in bold

River drainage	Elevation	Sample size	Unique haplotypes	*s*	Π	*k*	F_s
Merced	Low	53	20	84	0.025 ± 0.012	24.488 ± 10.928	5.699 $P = 0.942$
	High	48	11	76	0.023 ± 0.011	22.002 ± 9.867	14.859 $P = 0.998$
Tuolumne	Low	55	18	31	0.008 ± 0.004	8.068 ± 3.803	–0.271 $P = 0.497$
	High	25	10	7	0.001 ± 0.001	1.240 ± 0.812	–6.291 $\mathbf{P < 0.001}$

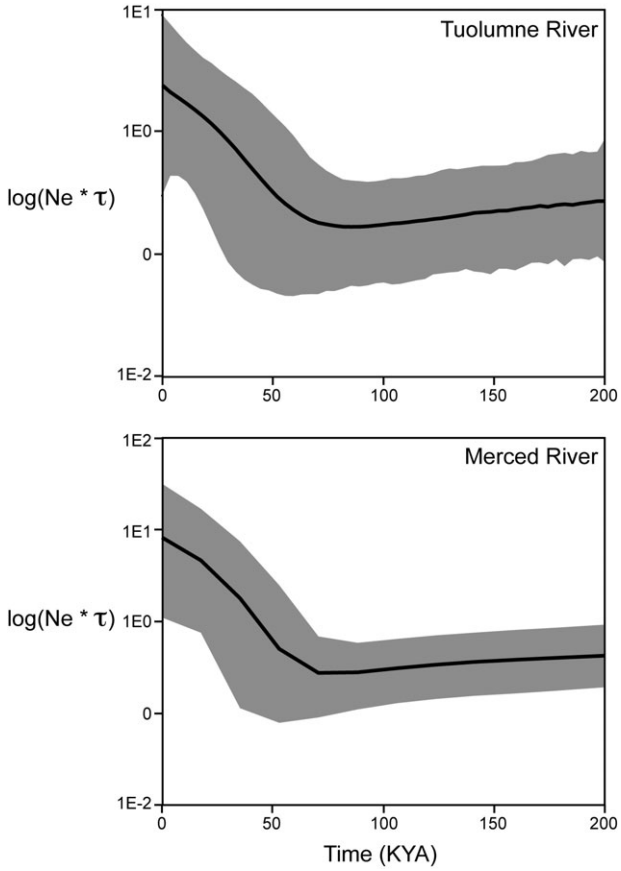

Figure 4. Bayesian skyline plots of population size changes through time. The median value for population size is tracked with a black line, the upper and lower 95% credible intervals are filled in grey. The time units are approximated using a 2% substitution rate per million years, and the population size axis is on the log-scale.

sion that some localities along the Merced River are sister to all remaining populations of *S. occidentalis*, including others from the Merced and those found along the Tuolumne River. Although this relationship is certainly supported in the context of our sampling scheme, a broad-scale phylogeographic study of *S. occidentalis* is necessary to place the mtDNA clades that we identified into a more comprehensive phylogenetic framework. On a smaller spatial scale, *S. occidentalis* exhibits a pattern of population genetic substructure associated with the Merced and Tuolumne river drainages that is similar to the pattern found in the Yosemite Toad, *Bufo canorus* Camp, 1916 (Shaffer *et al*., 2000). However, these geographic areas do not correspond to exclusive genealogical units, and we identified six instances of haplotype admixture between these areas. We found a preponderance of Tuolumne haplotypes in the Merced drainage, which could be taken as evidence for gene flow southward between drainages. Localities with admixed haplotypes occur at low-, mid-, and high-elevation localities (Fig. 2), suggesting that there is no correspondence between the mtDNA contact zones and elevation.

Demographic history

We predicted that *S. occidentalis* would show a signature of population expansion up the Tuolumne and Merced river drainages corresponding to the recession of the recent Tioga glaciation event (15 000–20 000 years ago). The presence of a deep phylogenetic break in *S. occidentalis* enabled a test of this hypothesis in two separate high-elevation lineages (clades A and B; Fig. 2). Genetic diversity was lowest across high-elevation populations along the Tuolumne River (Table 4), which is suggestive of recent expansion or high levels of gene flow. A population expansion in the Tuolumne River is also supported by Fu's F_s (Table 4) and the Bayesian skyline reconstruction (Fig. 4). In contrast, genetic diversity is relatively high for the high-elevation populations on the Merced River, and Fu's F_s is not significant for either high- or low-elevation populations along the Merced River (Table 4). However, the Bayesian skyline plot for the Merced River populations does support the hypothesis of recent population expansion (Fig. 4). Interestingly, the timing for the population expansions up the Merced and Tuolumne rivers is relatively recent (Fig. 4). Assuming a 2% substitution rate per million years places the timing of the population expansion to within the last 50 000 years, roughly consistent with the regression of the Tioga glaciation (up to 20 000 years ago). We acknowledge that this approach to molecular dating is highly speculative, and that the use of more precise dating techniques that incorporate multiple calibrations is desirable.

Sceloporus occidentalis is generally regarded as an abundant and widely distributed lizard, attributes that may facilitate high levels of interpopulation gene flow. However, this is not necessarily the situation throughout Yosemite because *S. occidentalis* is excluded from many dense conifer forest habitats at mid elevation, predominated by pines (*Pinus* sp.), where *S. graciosus* is common (A.D. Leaché, D.-S. Helmer & C. Moritz, pers. observ.). The distribution of *S. o. taylori* is especially patchy at high elevations, and they are generally restricted to exposed areas with substantial sun exposure (usually southward-facing slopes) with large boulders and rocks in the vicinity of Sierra juniper (*Juniperus occidentalis*). Thus, the possibility for extrinsic barriers to gene flow along elevation gradients, or among high populations, is strong given the current ecological and geological constraints on the distribution of *S. occidentalis* in Yosemite.

Phenotypic evolution

Body size differences among populations of *S. occidentalis* support a Bergmann's cline along elevation gradients in Yosemite, with high-elevation populations attaining a larger size compared with those at low elevations. Hatchling lizards at high elevation have fewer and shorter daily opportunities for food intake, which translates to lower growth rates and delayed maturation in colder environments (Sinervo & Adolph, 1994). These differences in thermal environments and maturation times can manifest as Bergmann's clines in body size along elevation and latitudinal gradients in *Sceloporus* (Angilletta *et al*., 2004, 2006). Laboratory studies of *S. occidentalis* collected from high- and low-elevation populations have demonstrated that population origin determines body size to a greater extent than phenotypic plasticity, which suggests a genetic component to body size differences (Buckley, Irschick & Adolph, 2010). However, populations of *S. occidentalis* from an elevation gradient in southern California do not show a Bergmann's cline, presumably as a result of gene flow among high- and low-elevation populations (Buckley *et al*., 2010). Thus, the complex and patchy distribution of *S. occidentalis* at high elevations in the Sierra Nevada may promote phenotypic divergence by impeding gene flow along elevation gradients.

The coupling of body size evolution with increased levels of blue ventral coloration in high-elevation populations is intriguing. High-elevation populations of *S. occidentalis* in Yosemite are darker in colour, which, similar to increased body size, is presumably an adaptation for coping with a more challenging thermal environment. In *Sceloporus*, the deposition of the pigment melanin is largely responsible for determining the darkness of the body (Morrison, Rand & Frost-Mason, 1995). The blue ventral coloration in *Sceloporus* is a structural colour reflected by iridophores, but an underlying melanin layer is required to absorb the remaining light to produce blue coloration (Quinn & Hews, 2003). Thus, the evolution of extensive blue ventral coloration in *S. occidentalis* may be a by-product of increased melanism in response to the more challenging thermal environment experienced by lizards at high elevations.

ACKNOWLEDGEMENTS

We thank the National Park Service for permission to conduct research and collect specimens in Yosemite National Park. We thank W. Brown, F. Burbrink. L. Clampitt, C. Conroy, T. Devitt, R. Hijmans, A. Leaché, D. Leaché, C. Linkem, J. McGuire, C. Spencer, and G. Wogan for field assistance. This manuscript benefited from comments provided by C. Conroy, J. McGuire, T. Papenfuss, J. Patton, R. Gillespie, and D. Wake. Funding was provided by the National Park Service and the Museum of Vertebrate Zoology, University of California, Berkeley.

REFERENCES

Angilletta MJ, Niewiarowski PH, Dunham AE, Leaché AD, Porter W. 2004. Bergmann's clines in ectotherms: illustrating a life-history perspective with sceloporine lizards. *American Naturalist* **164:** E168–E183.

Angilletta MJ, Oufiero CE, Leaché AD. 2006. Direct and indirect effects of environmental temperature on the evolution of reproductive strategies: an information-theoretic approach. *American Naturalist* **168:** E123–E135.

Brandley MC, Schmitz A, Reeder TW. 2005. Partitioned Bayesian analyses, partition choice, and the phylogenetic relationships of scincid lizards. *Systematic Biology* **54:** 373–390.

Buckley CR, Irschick DJ, Adolph SC. 2010. The contributions of evolutionary divergence and phenotypic plasticity to geographic variation in the western fence lizard, *Sceloporus occidentalis*. *Biological Journal of the Linnean Society* **99:** 84–98.

Burbrink FT, Lawson R, Slowinski JB. 2000. Mitochondrial DNA phylogeography of the polytypic North American rat snake (*Elaphe obsoleta*): a critique of the subspecies concept. *Evolution* **54:** 2107–2118.

Calsbeek R, Thompson JN, Richardson JE. 2003. Patterns of molecular evolution and diversification in a biodiversity hotspot: the California Floristic Province. *Molecular Ecology* **12:** 1021–1029.

Camp CL. 1916. The subspecies of *Sceloporus occidentalis* with description of a new form from the Sierra Nevada, and systematic notes on other California lizards. *University of California Publications in Zoology* **17:** 63–74.

Chapman AD, Wieczorek J. 2006. Guide to best practices for georeferencing. In: Chapman AD, Wieczorek J, eds. *Global biodiversity information facility*. Copenhagen: Global Biodiversity Information Facility, 1–80.

Clement M, Posada D, Crandall KA. 2000. TCS: a computer program to estimate gene genealogies. *Molecular Ecology* **9:** 1657–1659.

Drummond AJ, Rambaut A. 2007. BEAST: Bayesian evolutionary analysis by sampling trees. *BMC Evolutionary Biology* **7:** 214–221.

Drummond AJ, Rambaut A, Shapiro B, Pybus OG. 2005. Bayesian coalescent inference of past population dynamics from molecular sequences. *Molecular Biology and Evolution* **22:** 1185–1192.

Excoffier L, Laval G, Schneider S. 2005. Arlequin (version 3.0): an integrated software package for population genetics data analysis. *Evolutionary Bioinformatics Online* **1:** 47–50.

Excoffier L, Smouse PE, Quattro JM. 1992. Analyses of molecular variance inferred from metric distances among

DNA haplotypes: application to human mitochondrial DNA restriction data. *Genetics* **131:** 479–491.

Fu YX. 1997. Statistical tests of neutrality of mutations against population growth, hitchhiking and background selection. *Genetics* **147:** 915–925.

Huber NK. 1987. The geologic story of Yosemite National Park. *US Geological Survey Bulletin* **1595:** 1–64.

Leaché AD. 2010. Species trees for spiny lizards (Genus *Sceloporus*): identifying points of concordance and conflict between nuclear and mitochondrial data. *Molecular Phylogenetics and Evolution* **54:** 162–171.

Leaché AD, Cole CJ. 2007. Hybridization between multiple fence lizard lineages in an ecotone: locally discordant variation in mitochondrial DNA, chromosomes, and morphology. *Molecular Ecology* **16:** 1035–1054.

Leaché AD, Mulcahy DG. 2007. Phylogeny, divergence times and species limits of spiny lizards (*Sceloporus magister* species group) in western North American deserts and Baja California. *Molecular Ecology* **16:** 5216–5233.

Leaché AD, Reeder TW. 2002. Molecular systematics of the eastern fence lizard (*Sceloporus undulatus*): a comparison of parsimony, likelihood, and Bayesian approaches. *Systematic Biology* **51:** 44–68.

Moritz C, Patton JL, Conroy CJ, Parra JL, White GC, Beissinger SR. 2008. Impact of a century of climate change on small-mammal communities in Yosemite National Park. *Science* **322:** 261–264.

Morrison RL, Rand MS, Frost-Mason SK. 1995. Cellular basis of color differences in three morphs of the lizard *Sceloporus undulatus erythrocheilus*. *Copeia* **1995:** 397–408.

Mulcahy DG. 2008. Phylogeography and species boundaries of the western North American Nightsnake (*Hypsiglena torquata*): revisiting the subspecies concept. *Molecular Phylogenetics and Evolution* **46:** 1095–1115.

Nylander JAA. 2004. *MrModletest, version 2*. Program distributed by the author. Evolutionary Biology Centre, Uppsala University.

Nylander JAA, Wilgenbusch JC, Warren DL, Swofford DL. 2008. AWTY (are we there yet?): a system for graphical exploration of MCMC convergence in Bayesian phylogenetics. *Bioinformatics* **24:** 581–583.

Patterson TB, Givnish TJ. 2004. Geographic cohesion, chromosomal evolution, parallel adaptive radiations, and consequent floral adaptations in *Calochortus* (Calochortaceae): evidence from a cpDNA phylogeny. *New Phytologist* **161:** 253–264.

Quinn VS, Hews KD. 2003. Positive relationships between abdominal coloration and dermal melanin density in phrynosomatid lizards. *Copeia* **2003:** 858–864.

Rambaut A, Drummond AJ. 2007. *Tracer*. University of Oxford: Oxford.

Rissler LJ, Hijmans RJ, Graham CH, Moritz C, Wake DB. 2006. Phylogeographic lineages and species comparisons in conservation analyses: a case study of California herpetofauna. *American Naturalist* **167:** 655–666.

Ronquist F, Huelsenbeck JP. 2003. MrBayes version 3: Bayesian phylogenetic inference under mixed models. *Bioinformatics* **19:** 1572–1574.

Shaffer HB, Feller GM, Magee A, Voss SR. 2000. The genetics of amphibian declines: population substructure and molecular differentiation in the Yosemite Toad, *Bufo canorus* (Anura, Bufonidae) based on single-strand conformation polymorphism analysis (SSCP) and mitochondrial DNA sequence data. *Molecular Ecology* **9:** 245–257.

Sinervo B, Adolph SC. 1994. Growth plasticity and thermal opportunity in *Sceloporus* lizards. *Ecology* **5:** 776–790.

Smith HM, Bell ES, Applegarth JS, Chiszar D. 1992. Adaptive convergence in the lizard superspecies *Sceloporus undulatus*. *Bulletin of the Maryland Herpetological Society* **28:** 123–149.

Storer TI, Usinger RL, Lukas D. 2004. *Sierra Nevada natural history*. Berkeley: University of California Press.

Wiens JJ, Reeder TW, Montes De Oca, AN. 1999. Molecular phylogenetics and evolution of sexual dichromatism among populations of the Yarrow's Spiny Lizard (*Sceloporus jarrovii*). *Evolution* **53:** 1884–1897.

APPENDIX 1

Voucher specimens of *Sceloporus occidentalis* scored for body size and coloration. All specimens are deposited in the Museum of Vertebrate Zoology (MVZ), and specific locality data and GPS coordinates can be obtained from http://mvz.berkeley.edu/. Voucher numbers in the 5900 series correspond to specimens collected in 1915 during the original MVZ survey of Yosemite National Park. Body size and coloration data were collected for all specimens unless noted otherwise (C = coloration only; S = body size only).

Females ($N = 177$): 5935–7, 5940, 5942, 5946, 5949–50, 5957 (C), 240907–10, 240916–7, 240920–2, 240924–7, 240925–7, 240936–8, 240941 (C), 240950–1, 240959, 240961–2, 240963 (C), 240966, 240967 (S), 240968, 240970–2, 240976–7, 240985–6, 240989, 240993–4 (S), 241000–5, 241011, 241013, 241015–9, 241021–7, 241039–42, 241046–9, 241056–7, 241060 (C), 241062–3, 241068, 241071–3, 241076, 245615, 245631–6, 245639–42, 245646–8, 245651–2, 245655–6, 245661–2, 245669, 245672–8, 245682–3, 245685–6, 245688, 245693–5, 245698, 245703–4, 245708, 245712, 245715, 245719–21, 245724–5, 245730, 245735, 245737–8, 245742 (S), 245743, 245750–2, 245762–4, 245767, 245774, 245776, 245778–9, 245782, 245785, 245787–8, 250088–9, 250106, 250110–2, 250114, 250118–22, 250125–6, 250129, 250131–4, 250141–2, 250150, 250155–6, 250158, 250162.

Males ($N = 233$): 5859, 5863–4, 5934, 5938–9, 5941, 5944–5, 5947–8, 5951–56, 240905–6, 240911–15, 240918–19, 240923, 240928–35, 240942–9, 240952–8, 240960, 240964–5, 240969, 240973–5, 240978–84, 240990–2 (S), 240995–9, 241006–10, 241012, 241014,

241020, 241028–38, 241043, 241050–5, 241058–9, 241061, 241064–7, 241069–70, 241074–5, 245616–30, 245637–8, 245643–5, 245649–50, 245653–4, 245657–60, 245663–8, 245670–1, 245684, 245687, 245689–92, 245696–7, 245699–702, 245705–7, 245709–10, 245713–14, 245718, 245722–3, 245726–9, 245734, 245740–1, 245748–9, 245758 (C), 245760, 245765, 245770–1 (C), 245773, 245777, 245780–1, 245784, 245786, 245789–91, 250086–7, 250090–5, 250097–100, 250104–5, 250107–9, 250113, 250115–7, 250123–4, 250128, 250130, 250135 (C), 250137 (C), 250138, 250143–9, 250151–4, 250157 (C), 250159–61.

APPENDIX 2

Locality data and voucher specimen numbers for *Sceloporus occidentalis* included in the genetic analyses. All specimens are deposited in the Museum of Vertebrate Zoology (MVZ), and specific locality data and GPS coordinates can be obtained from http://mvz.berkeley.edu/. Locality numbers refer to labels used in the phylogenetic analysis and haplotype network.

(1) Hodgon Meadows (245580); (2) Evergreen Road, Stanislaus N.F. (241057); (3) Evergreen Road, Stanislaus N.F. (241059, 241062–3); (4) Hetch Hetchy Road (241043, 245734); (5) Hetch Hetchy Road (241056, 245747); (6) Hetch Hetchy Road (250135–6); (7) Hetch Hetchy Road (250138); (8) Hetch Hetchy, S. of Reservoir (241066); (9) Hetch Hetchy, N. of Reservoir (245776); (10) Hetch Hetchy, N. of Reservoir (250128); (11) Lake Eleanor (245773); (12) Rancheria Falls (250151, 250153–4); (13) Tuolumne River South Fork, Tioga Road (241058); (14) Lake Vernon (250124); (15) Lake Vernon (250133–4); (16) Lake Vernon (250141–4, 250147–8, 250158–9); (17) Hetch Hetchy, E. of Reservoir (245737, 245736); (18) Hetch Hetchy, E. of Reservoir (247739); (19) Hetch Hetchy, E. of Reservoir (245792); (20) Pate Valley (245779); (21) Pate Valley (245743, 245748); (22) Pate Valley (245762); (23) 7.5 miles West of Glen Aulin (241036, 241038–42); (24) Return Creek (241027–31); (25) between LeConte and Waterwheel Falls (241010–1, 241019–21); (26) between LeConte and Waterwheel Falls (241005, 241012–5); (27) California Falls (241006, 241009); (28) Glen Aulin (240999, 241001–4, 240991–4); (29) McGee Lake (241073–6); (30) Pothole Dome (245785–6, 245788–90); (31) Arch Rock, Yosemite Valley (240952–6); (32) Foresta (240919–22, 240907–10, 240948–50, 245641, 250094–5); (33) Wildcut Creek, Big Oak Flat Road (240962–6); (34) Cascade Creek, Yosemite Valley (245677); (35) Turtleback Dome (250089–92); (36) Yellowpine Camp, Yosemite Valley (245666); (37) 4–Mile Trail, Yosemite Valley (245622); (38) Mirror Lake Trail, Yosemite Valley (250110–1); (39) Happy Isles Nature Center, Yosemite Valley (240985–6); (40) Mirror Lake, Yosemite Valley (250115–7); (41) Yosemite Creek Campground (245724–30); (42) Yosemite Creek, Tioga Road (250086); (43) May Lake (245695–8, 245701); (44) Lake Tenaya (240932–6, 241045, 241048, 241051–4); (45) Olmsted Point (240925–8); (46) North Dome (25099–100, 245703–5); (47) Glacier Point (240972–7); (48) Little Yosemite Valley (245702, 245643, 245000); (49) Moraine Dome (245667); (50) Echo Valley (245682); (51) Merced High Sierra Camp (245656); (52) Lake Babcock (245706–9, 245637, 245640); (53) Washburn Lake (245615); (54) Wawona Campground (240911, 240913–6); (55) Chilnualna Creek, Wawona (240979–81); (56) Chilnualna Falls Trail, Wawona (240967, 250103, 250000).